Possible Mitigation of Global Cooling due to Supervolcanic Eruption via Intentional Release of Fluorinated Gases

Yangyang Xu[1], Nathanael P. Ribar[1], Gunnar Schade[1], Andrew Lockley[2], Yi Ge Zhang[3], Jeffrey T. Sachnik[1], Pengfei Yu[4], Jianxin Hu[5], Guus J. M. Velders[6,7]

[1]Department of Atmospheric Sciences, Texas A&M University, College Station, Texas, 77843, USA,

[2]Bartlett School, University College London, United Kingdom,

[3]Department of Oceanography, Texas A&M University, College Station, Texas, 77843, USA,

[4]Jinan University, Guangzhou, Guangdong, China,

[5]Peking University, Beijing, China,

[6]National Institute for Public Health and the Environment (RIVM), Netherlands,

[7]Institute for Marine and Atmospheric Research Utrecht (IMAU), Utrecht University, Netherlands

Corresponding author: Yangyang Xu (yangyang.xu@tamu.edu)

May 2023

Key Points:

- Several fluorinated greenhouse gases can reduce the magnitude of supervolcanic cooling to within natural variability.
- Radiative, physical and chemical properties of a hypothetical ideal compound can be estimated to mitigate specific volcanic cooling.
- Technical, economic and geophysical constraints and atmospheric chemistry consequences are discussed.

Abstract

Supervolcanic eruptions induced abrupt global cooling (roughly at a rate of ~1ºC/year lasting for years to decades), such as the prehistoric Yellowstone eruption released, by some estimates, SO_2 about 100 times higher than the 1991 Mt. Pinatubo eruption. An abrupt global cooling of several ºC, even if only lasting a few years, would present immediate and drastic stress on biodiversity and food production - posing a global catastrophic risk to human society. Using a simple climate model, this paper discusses the possibility of counteracting supervolcanic cooling with the intentional release of greenhouse gases (GHGs). Although well-known longer-lived compounds such as CO_2 and CH_4 are found to be unsuitable for this purpose, select fluorinated gases (F-gases), either individually or in combinations, may be released at gigaton scale to offset most of the supervolcanic cooling. We identify candidate F-gases (viz. C_4F_6 and CH_3F) and derive radiative and chemical properties of 'ideal' compounds matching specific cooling events. Geophysical constraints on manufacturing and stockpiling due to mineral availability are considered alongside technical and economic implications based on present-day market assumptions. The consequences of F-gas release in perturbing atmospheric chemistry are discussed in the context of those due to the supervolcanic eruption itself. The conceptual analysis here suggests the possibility of mitigating certain global catastrophic risks via intentional intervention.

1 Introduction

While the world is grappling with global warming, some have called attention to the risk of a much more abrupt global cooling due to natural or human causes (e.g., Robock et al., 2009; Coupe et al., 2019). At least three drivers of global cooling are global catastrophic risks (Bostrom and Cirkovic, 2008): thermonuclear warfare (Mills et al., 2014; Coupe et al., 2019), asteroid impacts (Vellekoop et al., 2014; Bardeen et al., 2017), and supervolcanic eruptions (Timmreck & Graf, 2005; Robock et al., 2009; Fendley et al., 2019; Black et al., 2021; Cassidy & Mani, 2022). All involve injections of absorbing and/or reflective materials into the upper atmosphere, reducing tropospheric and surface solar radiation flux. Consequently, global average surface temperatures would drastically decline over just a few years, gradually recovering as the injected materials deposit back to the surface.

For nuclear detonations, black carbon (soot) from urban firestorms is lofted into the stratosphere via efficient shortwave (SW) absorption and subsequent thermal transfer to and convection of the surrounding air mass (Coupe et al., 2019). Large asteroid impacts inject soot due to global forest firestorms and potentially also due to SO_2 released from vaporized crust near the point of impact. Ocean cooling following the bolide impact at the Cretaceous - Paleogene boundary (~66 Mya) was up to 7ºC along the Gulf coast (Vellekoop et al., 2014). The degree of cooling and the relative significance of cooling agents depend on factors such as the impact location and angle as well as the explosive power (Toon et al., 1997).

For supervolcanic eruptions, sulfur dioxide (SO_2) is released from crust/mantle rock at high temperatures. Intense heat within the volcanic plume results in convection into the stratosphere (Robock et al., 2009; Timmreck, 2012). In the stratosphere, SO_2 takes weeks to

form sulfate aerosols, which scatter SW radiation back to space, leading to surface cooling. For example, the 1815 Mt. Tambora eruption on the island of Sumbawa, Indonesia (Self et al., 1984) led to the subsequent "year without a summer" (1816). Such planetary scale events possess great destructive power and the potential to generate a global cooling at a rate of 1 ºC/year (Robock et al., 2009), which is about 100 times faster than contemporary global warming (on average less than 0.01 ºC/year since the industrial revolution). In comparison, CO_2 outgassing from volcanic eruptions contributed to paleoclimatic warming on a much longer timescale of centuries to millennia and only led to an even smaller warming rate (Black et al., 2018).

Though temperature recovery after such events could be on the order of a decade, ecosystems and human society would face major and potentially irreversible disruption. Agricultural yields, highly sensitive to changes in surface climate and solar insolation, would plunge worldwide (Scherrer et al., 2020; Da et al., 2021), likely resulting in the collapse of supply chains, subsequent civil disorder, and regional conflicts (Wilcox et al., 2015). It is, therefore, worth investigating preparation for potential mitigation.

Could global cooling events even be mitigated? Current thoughts mainly concern prevention. Concerns over a nuclear winter scenario were a catalyst for the 1980's arms treaties between the USA and the Soviet Union, but recent nuclear proliferation has caused renewed worries over regional wars (Coupe et al., 2019; Mills et al., 2014; Toon et al., 2014, Toon et al., 2019). Defense against asteroid impacts via early detection and kinetic redirection has been investigated (e.g., NASA's DART program), though recent studies suggest various extents of efficacy (Cheng et al., 2018; El Mir et al., 2018). By contrast, preparation for volcanic eruptions is primarily adaptive, with monitoring implemented to provide an early warning (potentially years ahead) for evacuation (Morton, 2021). Additionally, some engineering proposals to cool

subterranean magma chambers have been suggested (Wilcox et al., 2015; Denkenberger and Blair, 2018). However, such strategies may have the potential to induce phase changes within the chamber, enhancing hydrothermal explosions (Wilcox et al., 2015).

Anthropogenic warming, while associated with catastrophic risks itself, has inspired investigation into intentional climate intervention (geoengineering), such as Solar Radiation Management, which aims to lower global temperatures through space mirror deployment (e.g., Teller et al., 1997; 2002) or stratospheric aerosol injection (SAI; National Academy of Science, 2018) - which mimics volcanic cooling. "Counter-geoengineering" has also been discussed, considering injections of greenhouse gases (GHGs) to counteract SAI (Parker et al., 2018). The research question we consider here is: could deliberate releases of GHGs reduce the magnitude of supervolcanic cooling without subsequently producing undesirable consequences?

To address this question, global cooling due to a hypothetical supervolcanic 2 Gt SO_2 injection is simulated by a simple climate model here. This amount is similar in scale to the injection from the Yellowstone eruption (Timmreck and Graf, 2005) or a lower bound estimate of the Toba eruption (Robock et al., 2009), both of which were estimated to have a similar SO_2 injection rate and a Volcanic Explosivity Index (VEI) of 8. Our research extends Fuglestvedt et al. (2014), which used a global climate model to simulate the role of chlorofluorocarbons in offsetting the cooling due to the smaller Tambora eruption (with a VEI of 7; Newhall et al., 2018) by instead directly modeling a large suite of commercially available F-gases to identify potential offsetting candidates. Additionally, a brief discussion is offered on the geophysical, technical, and economic constraints on the production as well as the potential side effects on atmospheric chemistry. We do not recommend real-world preparations for deployment be taken soon; but instead, we intend to motivate further study and discussion regarding the proactive

mitigation of such global catastrophic risks, particularly those due to anthropogenic or natural climate changes.

2 Methods

2.1 Energy balance climate model

We utilize a zero-dimension energy balance model. This is inspired by Hasselman (1976) and was recently used by Ramanathan and Xu (2010), Xu and Ramanathan (2017), and Hanna et al. (2021). With the evolution of mass emission over a certain time interval as the desired model input, atmospheric concentration, top-of-atmosphere (TOA) forcing (Wm^{-2}), and surface temperature response (°C) are estimated.

For methane, CH_4, mass emission is used to derive concentration ($C(t)$; unit: parts per billion [ppb]) with the following equation (Eqn. 1).

$$C(t) = 715 + \left(\sum_{i=0}^{t} \frac{E[i]}{2.78} * e^{\frac{-(t-i-1)}{\tau}}\right) - \left(715 * \left(1 - e^{\frac{-t}{\tau}}\right)\right) \quad (1)$$

In Eqn. 1, E and t are the mass emission and time (in years) for a given year i, and τ is the e-folding lifetime of CH_4 (12 years per the Intergovernmental Panel on Climate Change [IPCC] Assessment Report 5 [AR5], assumed to be constant in this analysis). The conversion factor from the emission of 1 Mt to the atmospheric concentration of 1 ppb is 2.78 (ppb/Mt) (Table 7.6 in IPCC AR4 Working Group I [WGI]). We assumed a preindustrial concentration (to avoid considering the complexity of contemporary climate change) of 715 ppb (IPCC AR5) and natural emissions of 100 Mt per year.

The direct forcing of CH_4 has a square root relationship with concentration ($F_D(t)$ in Eqn. 2, ignoring the overlapping effect with N_2O since it is not modeled here), resulting in a marginally smaller response to concentration. The indirect forcings due to atmospheric chemistry, such as stratospheric water vapor (0.07 Wm^{-2}), formation of CO_2 (0.016 Wm^{-2}), and tropospheric ozone (0.2 Wm^{-2}), are smaller in magnitude. Thus, they are simply scaled here from the CH_4 concentration linearly (Eqn. 3-5, for stratospheric water vapor, CO_2, and tropospheric ozone, respectively). The coefficients are obtained from IPCC AR5 WGI, Chapter 8, as their separate contribution to the present-day (2005) forcing relative to the preindustrial (1850). The total forcing for CH_4 (F; unit: Wm^{-2}), on an annual basis (t), is then calculated in Eqn. 6.

$$F_D(t) = 0.57 * \left(\frac{\sqrt{C(t)}-\sqrt{C_{1850}}}{\sqrt{C_{2005}}-\sqrt{C_{1850}}}\right) \quad (2)$$

$$F_{I1}(t) = 0.07 * \left(\frac{C(t)-C_{1850}}{C_{2005}-C_{1850}}\right) \quad (3)$$

$$F_{I2}(t) = 0.016 * \left(\frac{C(t)-C_{1850}}{C_{2005}-C_{1850}}\right) \quad (4)$$

$$F_{I3}(t) = 0.2 * \left(\frac{C(t)-C_{1850}}{C_{2005}-C_{1850}}\right) \quad (5)$$

$$F(t) = F_D+F_{I1}+F_{I2}+F_{I3} \quad (6)$$

For the F-bearing compounds, the concentration can be estimated from the time-varying emission and molar mass:

$$C(t) = C(t-1) + (E(t) \times \alpha) - C(t-1) \times (1 - e^{-\frac{1}{\tau}}) \quad (7)$$

In Eqn. 7, E(t) is the emission amount at a given time step (in kt), and α is a mass conversion factor. The default time step is a day, considering their short lifetime of 0.5 to 3 years. Additional simulations using a longer time step of a month or a year were also tested for the shorter-lived Compound B (see below), which produced a high bias in concentration due to the omission of decay during the initial time step (the first month or the first year). The simulated concentration and forcing using a time step of a day and a month largely converged (see further discussion later). The conversion factor between mass emission and atmospheric concentration, α, is the mixing ratio of 1 kt emission (10^9 gram divided by m, which is molar mass in g/mol) with respect to the total molar count of the atmosphere. The final concentration is expressed in the unit of ppb, hence the multiplier of 10^9:

$$\alpha = \frac{\left(\frac{1e9\ g}{m}\right)}{\left(\frac{5e21\ g}{28.97 g/mol}\right)} \times 1e9 \quad (8)$$

The conversion to radiative forcing from the concentration is based on the radiative efficiency (Wm^{-2} ppb^{-1}) of the agents provided in Hodnerog et al. (2020). Some saturation in absorption bands could occur such that the linear relation could no longer be valid. If so, the GHG radiative forcing contribution will continue to increase, albeit at a lower rate. In that case, the necessary F-gas emissions estimated here will be biased low. However, the magnitude of this bias is difficult to quantify due to the lack of quantitative information in the literature.

In all cases (volcanic-related emissions, CH_4, and F-gases), we regard the forcing numbers as the instantaneous forcing at the TOA without considering the fast adjustment of clouds and stratosphere (effective radiative forcing). The total forcing generated by all compounds will collectively drive the temperature response using the following equation:

$$T(t) = T[0] + \sum_0^{i_t}\left(\frac{1\,year}{C_p \times \rho \times z} \times \left(F[i] - \frac{T[i]}{s}\right)\right) \quad (9)$$

where T and F are the temperature and forcing for a given year; C_p and ρ are the specific heat and density of seawater; z is the depth of the effective ocean mixed layer; s is climate sensitivity expressed in the unit of °C/(Wm^{-2}). The time step in Eqn. 9 is adopted to be one year. We tested the sensitivity to the time step assumption in Ramanathan et al. (2022) (one year vs. one month) in the context of global climate mitigation in the next few decades, and the results using different time steps were consistent. We do not directly implement the shorter (daily or monthly) time steps in the forcing-temperature response function of Eqn. 9 for three reasons. First, the radiative forcing formulation (concentration and forcing for CH_4 and F-gas) is based on empirical approximation at an annual mean (and global average) basis after accounting for the seasonal dependence of the background thermal radiation from the Earth that would affect the radiative efficiency. Second, the literature does not provide a supervolcanic forcing time series in the necessary daily or monthly resolution. Third, the emission rate of F-gas is estimated to match the annual mean supervolcanic forcing. Therefore, any bias in quantifying temperature response using the energy balance equation would operate equally in both the warming and cooling case and does not directly affect the emission estimates.

Regardless, as a robustness check, we implement the shorter time step (daily or monthly) in the emission-concentration relationship (Eqn. 7) in one case. After obtaining the concentration at the daily or monthly resolution, we convert it to an annual mean with a running average before quantifying its radiative forcing (using the formulations constructed on an annual mean basis) and temperature response (using Eqn. 9 at the annual time step). This is presented in Figure 6.

211

212 2.2 Validation of the climate model

213 The 1991 eruption of Mt. Pinatubo injected ~20 Mt SO_2, the effects of which have been
214 closely observed and extensively studied (Stenchikov et al., 1998; Ramachandran et al., 2000;
215 Soden et al., 2002). Observations from Pinatubo are used to test model fidelity (Figure 1),
216 specifically the conversion of eruption-driven radiative flux anomalies into global average
217 temperature response.

218 Using observed monthly mean SW and longwave (LW) flux anomalies (covering only
219 60°S-60°N), the annual average of total TOA (top of atmosphere) forcing is calculated and input
220 into the model (Figure 1a). The effective ocean mixed layer depth (z in Eqn. 9) is assumed to be
221 relatively small (35 m) to reflect the short temporal scale of the Pinatubo eruption and the limited
222 role of oceanic thermal inertia. The simulated cooling largely agrees with the observed global
223 average temperature drop of approximately 0.4 °C at Year 2, with a recovery curve also aligning
224 closely with published data (Figure 1b) (Soden et al., 2002; Bender et al., 2010).

225 The model was also used to simulate the temperature response to a 2 Gt SO2 emission
226 scenario with a prescribed forcing (Figure 2a; Robock et al., 2009). While the prescribed forcing
227 in Robock et al. (2009) might be an overestimate according to other studies (Timmreck et al.,
228 2010; Lane et al., 2013; Smith et al., 2018; Black et al., 2018), this model also tracks Robock et
229 al.'s published temperature response well, which was derived using a more complex global
230 climate model. Here we used a configuration of z=50 m and s=0.45 °C/(Wm^{-2}) for the five years
231 post-eruption (Figure 2b). The effective ocean mixed layer depth (z) of 50 m is a reasonable
232 assumption given the short duration of the forcing, and agrees with Fuglestvedt et al. (2014) who
233 adopted a slab ocean model with a fixed depth of 54 m. The smaller climate sensitivity of 0.45

234 °C/Wm^{-2} is used, presumably because some positive climate feedback, such as ice-related
235 surface albedo feedback, is not fully involved at a short timescale of 1-5 years.

236 The lack of a second (deeper) ocean box neglects the increasing role of the ocean in
237 buffering the forcing and thus makes the recovery too quick compared to Robock et al.'s coupled
238 climate model. Our recent works (Ramanathan et al., 2022; Chen et al., 2021; Chen et al., 2020)
239 used a two-box energy balance model with a coupled carbon cycle. Since CO_2 emission is not
240 directly relevant to this paper, we use the simpler 1-box model over the 2-box configuration.
241 This 1-box model has also been used and validated extensively (Dreyfus et al., 2022; Xu and
242 Ramanathan, 2017; Xu et al., 2013). Previous careful comparisons with the two-box version and
243 the more complex MAGICC model have been made (Hanna et al., 2021). Therefore, the utility
244 and limitations of the 1-box model are well documented and justify its application here.

245 To fully demonstrate model sensitivity to the role of ocean heat content in buffering the
246 response to forcing, Figure 2b shows temperature response assuming a larger effective ocean
247 layer depth (80 meters) after Year 5, which produces a better fit to the coupled ocean-atmosphere
248 global climate model results. Similar to the concern of time step issues addressed in Section 6.2d,
249 the assumption of effective ocean mixed layer depth (z) does not directly affect the derivation of
250 required F-gas emission since the F-gas warming will also be prolonged by the same fraction
251 with a larger z and a close match with the volcanic radiative forcing will be maintained.

252

253 2.4 OH decay rate perturbation due to fluorinated gases (F-gases)

254 The enhanced decay rate of OH (in s^{-1}) due to a specific F-gas is estimated using
255 (d[OH]/dt)/[OH] = - k(F-gas)*[F-gas], where [OH] and [F-gas] is the molecular density (number
256 of molecules per cm^3) and k(F-gas) is the reaction rate constant in cm^3/molecules/s. k(F-gas) is

estimated by 1/(lifetime*[OH]) without considering temperature dependence, where the average global [OH] is ~10^6 molecules/cm^3 (Brasseur et al., 1999). [F-gas] is calculated from the mixing ratio multiplied by atmospheric molecular density (~$2.5*10^{19}$ molecules/cm^3). The background OH decay rate, primarily due to atmospheric CO and CH_4, is similarly estimated, based on [CO] and [CH_4] as well as k(CO) and k(CH_4) (Brasseur et al., 1999).

3. Results

3.1 Simulated cooling in response to supervolcanic eruption

A supervolcanic cooling event (e.g., with a VEI of 8) has not been observed in recent history, so any associated analysis must rely on mass flux approximations. Robock et al. (2009) presented a range of estimates for the Toba eruption 74,000 years ago, highlighting 6 Gt SO_2 (300x Pinatubo) as "most likely". This study considers the lower estimate of 2 Gt (100x Pinatubo) in Robock et al. (2009), close to assumptions in Timmreck and Graf (2005) for Yellowstone. Recent work has uncovered two previously unknown supereruptions from Yellowstone, the largest of which (Grey's Landing, 8.7 Ma BP) is 11% larger than the second-largest (Huckleberry Ridge, 2.1 Ma BP) (Knott et al., 2020; Timmreck and Graf, 2005). Thus, the mass emissions for supervolcanic eruptions such as Yellowstone and Toba are highly uncertain, and a determination of the actual magnitude is beyond the scope of this work.

Since our energy balance model cannot resolve the troposphere and stratosphere, forcing estimates from previous 3D modeling are used (Robock et al., 2009). A large 50 Wm^{-2} TOA forcing (Figure 2a) is converted from the surface SW forcing time series presented in Figure 4 of Robock et al. (2009). The conversion is needed because of the offset of the LW warming effect

of volcanic aerosols and stratospheric solar absorption. The conversion factor of 0.5 (Net_TOA/SW_surface) is estimated from the numbers in Figure 5 by Timmreck et al. (2005) and Table 2 by Timmreck et al. (2012), suggesting a ratio of 0.4 to 0.6. Volcanic particulate matter, CO_2, and H_2O emissions have been neglected here. CO_2 emissions, even from large volcanic eruptions, have small impacts on the timescale of years to decades (Timmreck et al., 2012; Ramachandran et al., 2000).

In response to a Yellowstone-like 2 Gt SO_2 injection, fossil records show a high survival rate of African megafauna and Indian hominids, implying more limited cooling than previously predicted (Timmreck et al., 2012). Modeling with detailed microphysical processes of formation and growth of sulfate aerosols (Timmreck et al., 2010; Timmreck et al., 2012) suggests a third of the cooling assumed by Robock et al. (2009). Forcing estimates in Robock et al. (2009), as adopted here, are thus considered likely overestimates due to omitting sulfate aerosol size distribution dependence (Timmrick et al., 2012). Nevertheless, our main purpose is to determine whether the concept of F-gas injection is generally feasible rather than targeting any particular cooling scenario. Forthcoming studies may address more realistic scenarios, including the uncertainty of forcing magnitude and temporal sequences.

Figure 2b shows a simulated plunge in the global annual average temperature of more than 10 °C following a 2 Gt SO_2 injection into the upper atmosphere. The cooling decreases after three years, and the temperature gradually recovers to within 1°C of the initial climate state approximately a decade after the eruption - emulating 3-D global climate model outputs (dashed line in Figure 2b). Temperatures rebound as coagulation and fallout of stratospheric sulfate aerosol occurs. Given its magnitude, the comparatively short cooling period can still be globally disastrous, e.g., due to net primary productivity decline. Cooling could be prolonged if volcanic

303 eruptions cluster over a long or even geologic period, with continental flood basalt events (e.g.,
304 Siberian and Deccan Traps) being extreme examples (Sayyed, 2013).

305 The discrepancy between this model and Robock's global climate model estimates as the
306 temperature recovers (Figure 2b, after Year 6) is possibly due to fixing effective ocean mixed
307 layer depth (z) as a constant throughout our simulation rather than allowing it to increase (as
308 inherently in global climate models where a deeper ocean would carry more heat inertia and
309 therefore make the recovery from the imposed forcing slower). This model sensitivity is
310 demonstrated in Figure 2b (see Methods Section). This model limitation, while not directly
311 affecting the main results in the later section on the required magnitude of F-gas emissions, will
312 need to be improved in future analyses, especially when considering the forcing sequence (e.g.,
313 multiple subsequent eruptions).

314 To fully comprehend the large forcing and cooling rate here, we first consider the
315 possibility of directly releasing natural gas. Its main constituent, CH_4, has a GWP100 of 28
316 (global warming potential over 100 year time scale being 28 times larger than CO2) and a
317 GWP20 of 84 (IPCC AR5). Figure 3a shows this scenario; the required mass release of CH_4 is
318 very large (200 Gt vs. current natural gas production of ~2.9 Gt/year (3.8 trillion cubic meters;
319 IEA, 2021). Figure 3a shows that injected CH_4 cannot avoid "overshoot" as the initial success in
320 offsetting the supervolcanic cooling (despite an unrealistically high emission requirement) is
321 followed by an overheating of more than 5 ºC for many years, which would also be disastrous.
322 The decadal lifetime of CH_4 is too long to counter abrupt but temporary cooling. Moreover, the
323 actual CH_4 lifetime under such a large release would be even longer due to an associated
324 reduction of atmospheric OH levels in response to the CH_4 injection (the primary CH_4 sink).

Matching the required response time of the forcing and the lifetime of warming agents is central to the selection of candidate gases. As a model sensitivity exercise, the CH_4 lifetime was lowered to 2 years. Radiative efficiency was simultaneously increased by 35 times to 0.027 $Wm^{-2}ppb^{-1}$, testing if the required mass release can be lowered correspondingly. The simulated temperature response obtained is encouraging. The temperature response curve of this "unstable and short-lived" designer compound (Figure 3b) is opposite to the supervolcanic cooling with comparable magnitude and achieved at a much lower emission rate of 6 to 3.5 Gt in Years 1 and 2. This exercise prompted an examination of other existing short-lived compounds with higher radiative efficiency.

3.2 Temperature responses to F-gas injections

Fluorinated gases (F-gases) have been known contributors to global warming since the latter half of the 20th century, with radiative forcing equivalent to 18% of CO_2, despite concentrations at least six orders of magnitude smaller (Hodnerog et al., 2020). These compounds are widely used as refrigerants, fire suppression agents, and for blowing foam insulation (Velders et al., 2015). Most are non-toxic, non-flammable, and non-reactive., Other F-gases – especially HFCs – have increased in production after the agreement of the Montreal Protocol in 1987, which phased out the use of ozone-depleting Cl- and Br-bearing F-gases (CFCs, HCFCs, Bromocarbons) (Velders et al., 2009). The increased use of HFCs is also a target of climate mitigation for the 21st century (Xu et al., 2013; Velders et al., 2015; UNEP & IEA, 2020).

HFCs have a wide range of atmospheric lifetimes (from months to 40 years) and global warming potentials (GWP100 ranging from <1 to 4,790) (Hodnerog et al., 2020). Analysis of

348 CH_4 (Section 2) suggests shorter lifetimes and higher radiative efficiencies are needed. Thus, in
349 our selections, we deliberately exclude compounds with lifetimes longer than 3.5 years to
350 mitigate the issue of persistent overheating. Excluding compounds with lifetimes below 0.5 years
351 (reactive halogens, typically ranging from days to weeks) avoids the requirement for near-
352 continuous releases. Ozone-depleting Br- and Cl-bearing gases and those containing oxygen
353 atoms (due to their more complex structures) were also excluded from the analysis. Table 1 lists
354 the resulting potential candidates selected from the 5-page-long Table 5 in Hodnerog et al.
355 (2020).

356 The candidates in Table 1 were further narrowed by selecting those with a higher
357 GWP100/lifetime ratio (rightmost column). GWP100/lifetime was used as the ranking criterion
358 over GWP100 for multiple reasons. First, GWP100 represents integrated forcing (akin to
359 temperature response) over 100 years. Second, GWP100/lifetime is sensitive to both radiative
360 efficiency and lifetime, as opposed to only radiative efficiency. And third, GWP100 alone does
361 not closely correlate with near-term warming (a few years after emission), the focus of this
362 study. Assuming the same radiative efficiency and molar weight, the same instantaneous mass
363 release will last longer in the atmosphere with a longer lifetime and will produce larger warming
364 over 100 years (hence a larger GWP100).

365 The release of the top five compounds was modeled separately. The model was run
366 numerous times for each compound, with the magnitude and timing of emissions adjusted after
367 each run to approach a minimized temperature residual - defined as within a +/- 1 °C range of the
368 pre-eruption level throughout the entire post-eruption recovery (Figure 4a-e). We discuss the
369 properties of these five identified compounds below, ordered by GWP100/lifetime ratio (Table
370 1).

371 Compound A, C_4HF_5 (Pentafluoro-cyclobutene in Figure 4a), has a lifetime of 0.7 years;
372 and a GWP100 of 97. Emission deployment after optimization is 6.0 Gt in Year 1 and 6.5 Gt in
373 Years 2-3 (Figure 5a), distributed evenly over 365 days of a year. The response residual after
374 mitigation is in the range of -1.4 to 0.9 °C (Figure 5b). Its lowest GWP (among the five
375 compounds tested here) and shortest lifetime necessitate a greater amount of total emissions to
376 offset the specific cooling.

377 Compound B, C_4F_6 (Hexafluoro-cyclobutene in Figure 4b), has a lifetime of 1 year and a
378 GWP100 of 132. In order to offset the cooling, it requires an emission deployment of 8.25 Gt in
379 the Year 1 post-eruption, followed by 2.75 Gt in Years 2-3 (Figure 5a). This is a promising
380 candidate, offsetting the cooling almost entirely, with the residual falling within a 1ºC level
381 (Figure 5b).

382 Compound C, CH_3CHF_2 (HFC-152a in Figure 4c), has a lifetime of 1.6 years and
383 GWP100 of 172. The optimized emission sequence is 5.6 Gt in Year 1 and 5.5 Gt in Year 2.
384 Similar to C_4F_6, HFC-152a can greatly offset cooling with a slightly less massive emission,
385 maintaining a residual below ±1 °C.

386 Compound D, $CH_2FCHFCF_3$ (HFC-245eb in Figure 4d), has a lifetime of 3.2 years and a
387 GWP100 of 341. It only needs a single-year release of 6.75 Gt in Year 1 alone. The longer
388 lifetime and larger GWP enable the least amount of total mass release. However, the temperature
389 response residual is less ideal (in contrast to A with the shortest lifetime) and can be as large as
390 1.3 to 2.6°C.

391 Compound E, CH_3F (HFC-41 in Figure 4e), has a lifetime of 2.8 years and GWP100 of
392 142. This compound requires the largest release rate (16 Gt in Year 1, 1.5 Gt in Year 2) due to its
393 low radiative efficiency (an order of magnitude smaller than Compound D of HFC-245eb, Table

1). This deficiency is offset by a longer lifetime, hence the relatively large GWP. Although the temperature residual is one of the least ideal among other compounds, its chemical simplicity may imply smaller production costs and environmental effects (see Sections 4 and 5).

Compounds with lifetimes below 2 years (A, B, C) and higher GWP/lifetime ratios offer more satisfactory emission sequences and temperature residuals (Figures 4 and 5). Moreover, C_4F_6 and HFC-152a both reduce the eruption-induced cooling to within a 1°C range for the entire duration of the experiment period. In contrast, the lower GWP/lifetime ratios in D and E produce undesirable cooling and warming due to excessive lifetime. This is especially apparent for HFC-245eb in Figure 4d, despite it having the highest GWP of the tested compounds.

Additionally, the metric of integrated radiative forcing can be used to interpret the temperature response to diverse compounds (Figure 6). Radiative forcing (Figure 6b) and integrated radiative forcing (Figure 6c) are shown for two representative F-gases with similar GWP (to contrast with the volcanic forcing also plotted in Figures 6b and c). Total mass releases of HFC-41 and C_4F_6 are 14 Gt and 8.3 Gt, respectively, despite having similar GWP (142; 132). The resulting volume concentrations are different by roughly an order of magnitude (Figure 6a) due to HFC-41's much smaller molar weight. However, both instantaneous and integrated radiative forcings are similar, given C_4F_6's larger radiative efficiency (Table 1).

Clearly, the integrated radiative forcing in Figure 6c can approximate the temperature counterbalance well for short-lived gases. The difference in temporal response is also consistent with the temperature simulation in Figure 4. For example, HFC-41 (red) shows an initial underheating followed by an overheating (Figure 6c). C_4F_6 maintains a closer mirroring of integrated forcing with respect to volcanic eruptions (Figure 6c, blue)—also shown in the match of temperature trajectories up to Year 4, after which an under-compensation is found.

While these five shortlisted compounds show promise in mitigating most of the cooling, they are designed and manufactured for different purposes and are clearly not ideal. We lastly discuss the possibility of a designer compound (Figure 4f) that can be tuned to produce almost exactly the desired cooling mitigation (residual <0.5 ºC) – statistically indistinguishable from interannual climate variability. As an exploratory exercise, this 'ideal' compound is speculated to possess the largest radiative efficiency of 0.3 $Wm^{-2}ppb^{-1}$ found in C_4F_6 (Figure 4b), while maintaining a small molar weight of 67 similar to HFC-152a (Figure 4c). Fine-tuning the mass emission sequences to achieve the right amount of warming (Year 1-4 at 2.75 Gt, 2.25 Gt, 0.75 Gt, and 0.5 Gt, respectively; the rightmost bar in Figure 5a) suggests a lifetime of ~0.9 years — between that of C_4HF_5 (Figure 4a) and C_4F_6 (Figure 4b). While we refrain from making recommendations on the elemental composition and molar structure, the identified characteristics (molar weight, radiative efficiency, and lifetime) above are similar to those existing, suggesting the possibility of designing an 'ideal' compound mixture.

4 Discussion

4.1 Geophysical, technical, and economic limitations

Fluorine used to manufacture F-gases is extracted from mined fluorspar (CaF_2) and fluorapatite ($Ca_5(PO_4)_3F$) ores. Post-extraction, these minerals are directly refined (fluorspar) or chemically converted (fluorapatite) into pure CaF_2, the primary material in the production of F-bearing gases (Jaccaud, 2020). There is an estimated 5 Gt of CaF_2 equivalent extractable reserve on the Earth (USGS, 2020), about 2.5 Gt of F-equivalent. Based on our calculation, HFC-245eb requires the least amount of elemental fluorine (70% of its total mass), about 4.2 Gt in total (all

needed in Year 1). Yet, this elemental fluorine mass is still at least three orders of magnitude larger than the present-day production of about 7 million tons annually (Hayes et al., 2017).

The required production would consume nearly all of the currently estimated global CaF_2 reserves, but mineable reserves may increase with future exploration. This constraint may be alleviated by tapping into the ocean-based source. Approaches to extracting dissolved F ions from the ocean exist (Tressaud, 2008), but a close examination of technical details and costs is beyond the scope of this paper. The fluorine content of seawater ranges between 1 and 1.4 mg/L (Jaccaud et al., 2020). Presuming a mineable shallow (300 m) surface ocean with a volume of roughly 100 million km^3, up to 150 Gt of fluorine could be extracted, far more than the required F mass of the single-digit Gt scale.

Jaccaud et al. (2020) placed the price of elemental fluorine (F, molar weight = 19 g/mol) at $5-8 per kilogram, based on extracting from mineral sources only, not the ocean. As a rough estimate, adopting the value of $5 per kilogram (presuming future economies of scale) and doubling this cost for incorporation into the HFC, manufacturing the compound with the smallest F requirement out of the five compounds tested (HFC-245eb), 4.8 Gt during deployment, would cost a total of 48 trillion dollars, twice the modern US GDP — an exercise justifiable as an alternative to global calamity.

Considering the lead time for scaling up production capacity, studies have shown that extreme magnitude eruptions are likely preceded by some geologic signals (Wilson et al., 2021), providing possible predictability. However, given the limited monitoring capacity and unknown factors contributing to eruptive timing and magnitude, the range of lead times is wide - from days to decades (Wilson et al., 2021; Morton, 2021). In an optimistic scenario with ample lead time, F-gas stockpiles could be, in principle, manufactured in advance. Such an enormous

accumulation of F-gas would be an inarguably complex project, accompanied by similarly complex economic, engineering, and security concerns. A thorough cost-benefit analysis would require in-depth collaboration between climatologists and experts in these fields, which is beyond this proof-of-concept study.

This analysis identified properties of a single candidate; however, a cocktail of novel "designer" compounds (fluorinated or not)—with enhanced absorption efficiency, mixed lifetimes, and reasonable production cost—could be developed and manufactured. Similar proposals exist in the context of geoengineering (Cao et al., 2017) and counter-geoengineering (Parker et al., 2018). Future, detailed analyses to assess such strategies' technological and economic feasibility are anticipated.

4.2 Chemical consequences

Gigaton-scale releases of compounds containing C-H bonds, coupled with a marked decline in solar radiation reaching the troposphere, could also disrupt the tropospheric chemistry of the hydroxyl radical (OH). A large depletion of tropospheric OH as a major chemical sink, especially in the boundary layer near surface release points, could exacerbate air pollution issues due to primary emissions of CO and VOCs by increasing their lifetimes. The OH loss rate due to F-gases can be calculated and compared to the loss rate due to background CH_4 and CO abundance at ~1 s^{-1} (Methods; Brasseur et al., 1999). Our model estimates approximately a 100 to 150 ppb initial abundance of C_4F_6 after release and instantaneous dilution (Figure 6a) – equivalent to a 0.1 to 0.15 s^{-1} OH reactivity. This is equivalent to a 10-15% drop from the background, which can significantly increase CH_4 lifetime. Reductions in OH due to F-gas oxidation followed by an increase in the lifetime of background CH_4 would induce additional

warming, implying less F-gas is needed. In the case of CH_3F (HFC-41), our calculation (Figure 6a) shows that the average tropospheric mixing ratio would be as high as 2000 ppb, which could create an OH loss rate of ~0.6 s^{-1}, more disruptive than C_4F_6. However, even assuming the 60% drop in OH decay rate and subsequent CH_4 lifetime increase, this would only lead to a rough doubling of CH_4 concentration from the background level. Following Eqn. 6, this translates to about an increase of 0.5 Wm^{-2}, almost two orders of magnitude smaller than the direct forcing from F-gases (Figure 6b).

Chemical interactions between F-gas releases and volcanic SO_2 emissions could lead to secondary effects on atmospheric chemistry. F-gases may alter SO_2 and sulfate lifetimes, with consequences for cooling and recovery timeline. The oxidation of released F-gas could lead to slower SO_2 oxidation (due to lower OH levels) to form sulfate aerosols and thus mute the volcanic cooling response, similar to the competing effects of a large volcanic eruption itself leading to slower SO_2 oxidation (Stevenson et al., 2003). Dynamically, the tropospheric warming due to F-gases may alter the circulation pattern that changes the lifetime of stratospheric aerosols. These complex chemical and dynamic interactions are not yet included in the simple climate modeling analysis reported herein.

Other adverse environmental and health impacts could result from first or second-order F-gas reaction products, which may be toxic. FHCO, the first reaction product of CH_3F, may accumulate near release sites; its aqueous formation of HF could have health and environmental effects due to gas-phase exposure or acid rain. Due to these ecological risks, the impact needs to be mitigated by monitoring and facilitating the mineralization of fluorine upon degradation from the injected gases. Adverse perturbations to biogeochemical cycling need to be placed in the context of the supervolcanic eruption, which would have already significantly disrupted the

stratospheric ozone layer and tropospheric chemistry, followed by acid rain and tropospheric haze due to aerosol fallout.

4.3 Limitation on spatially balanced temperature response

Despite successfully rebalancing global mean temperature using F-gas releases, a mismatch in spatial distribution is likely (Fuglestvedt et al., 2014); relative underheating is found in the tropics, where aerosol-induced cooling is stronger than at higher latitudes (Fuglestvedt et al., 2014). Vertically, some overheating is possible in the stratosphere, where volcanic aerosols lead to strong local heating, warming of the tropopause, and disruption of typical stratospheric dynamics. These spatial mismatches are also known issues for SAI, and potential fixes have been proposed via a strategic release in a specific latitude, altitude, and season (Tilmes et al., 2017; Tilmes et al., 2018; Visioni et al., 2019; Xu et al., 2020). A similar strategy with multi-location (varying different latitudes) surface release could be employed with F-gases, given their similarly short lifetimes. More complex modeling strategies must be used to test these possibilities, such as energy balance models with higher dimensions (North & Kim, 2017) or a global climate model (Fuglestvedt et al., 2014).

Fuglestvedt et al. (2014) used a global climate model with a spatial resolution of 1.9°x2.5°, providing valuable insights into regional and hydrological impacts; however, it was not suited for screening candidate compounds due to computational resource constraints. This analysis also advances beyond Fuglestvedt et al. (2014), because the previous study only considered a much smaller eruption (3x the magnitude of the 1991 Pinatubo eruption) and a single hypothetical compound (with radiative properties equivalent to CFC-11 but a shorter

lifetime and no impact on stratospheric ozone) and it only discussed side effects such as stockpile leakage very briefly (see their p. 14).

5. Conclusion

Super volcanic eruptions can lead to abrupt global cooling for years to a decade. The disruption to food production and social systems would be enormous and is considered a potential global catastrophic risk. This modeling study analyzed the possibility of releasing selected greenhouse gases to offset global cooling due to volcanic aerosols. We examined a suite of commercially available F-gases with varying radiative efficiency and lifetime and identified a few leading candidates for such an undertaking (Table 1). Specifically, we examined the suite of F-gases in Hodnerog et al. (2020) with lifetimes between 0.5 and 3.5 years to avoid the issues of persistent overheating and continuous deployment. Br and Cl-bearing gases were excluded due to ozone depletion, as well as those containing oxygen due to their more complex structure. Selected gases would need to be manufactured, stocked, and released at Gt-scale to counterbalance a Yellowstone-like super volcanic eruption. We found that even after such a large-scale eruption, the residual temperature changes could be kept within typical year-to-year natural variability. The desired physical and chemical properties of an 'ideal compound' were identified, which would almost completely offset the known cooling when released in subsequent years after the eruption. The actual selection of a compound to combat a super volcanic eruption and the necessary mass release of this compound is dependent on the specific volcanic cooling. Longer-lived greenhouse gases such as methane are clearly not fit for purpose due to the short-term nature of volcanic cooling.

While ‘ideal’ compounds (or their combinations) with Gt-scale release appear to be capable of offsetting the volcanic cooling, detailed discussions on the limitations and caveats of this approach are offered. These include the production limitations due to the geophysical constraints on mineral availability, as well as the technical and economic constraints (estimated based on the current market). While it is possible that future technology development can relax some of these constraints, the environmental consequences of massive F-gas release, both on the perturbation to the atmospheric oxidation capacity and precipitation acidification, and also on the spatial pattern of temperature responses need further scrutiny. However, these side effects may be tolerable in comparison to the immense consequences of unmitigated cooling.

The analysis presented here suggests global catastrophic risks due to abrupt cooling could at least be partially mitigated with artificial approaches. Due to the prototypical nature of this analysis, here we do not suggest real-world deployment in the near future. Producing massive amounts of F-gas seems to be limited by land-based mineral availability, and further economic analysis is hindered by the technical uncertainty in oceanic extraction. Moreover, due to the large uncertainty of cooling magnitude, preemptive manufacturing and large-scale stockpiling are needed. Still, no assessment is available on technical solutions for transport and storage, as well as associated risks such as inadvertent leakage.

This study advances the necessary discussion regarding the proactive mitigation of global catastrophic risks and aims to inspire more research in this direction. Similar concepts were presented in the literature, at least qualitatively, such as releasing GHGs or heating aerosols as counter-measures in response to unilateral solar-radiation geoengineering (Parker et al., 2018) or injecting substances that bind to sulfate aerosols to reduce their atmospheric lifetime in response to supervolcanic eruptions (Cassidy and Mani, 2022). Others considered volcanic eruption

prevention via direct cooling of subterranean magma chambers (Wilcox et al., 2015; Denkenberger and Blair, 2018). To safeguard the long-term continuity of human civilization, such forward-thinking should not be restricted (which is unfortunately argued for in Biermann et al. 2022).

Acknowledgments

We are grateful for the comments and encouragement from Drs. Gabrielle Dreyfus, Gerald North, Zachary McGraw, and Brian Toon. The analysis is supported by a National Science Foundation supplement fund (#1841308) for Research Experience for Undergraduate students. Nathanael Ribar acknowledges the programmatic support from the Texas A&M University Undergraduate Research Scholars program.

Open Research

All underlying data needed to understand, evaluate, and build upon the reported research, as well as the Python code for the modeling and data analysis, will be openly shared upon acceptance and publication.

References

Archer, David, et al. "Atmospheric Lifetime of Fossil Fuel Carbon Dioxide." *Annual Review of Earth and Planetary Sciences*, vol. 37, no. 1, 2009, pp. 117–134., https://doi.org/10.1146/annurev.earth.031208.100206.

Bardeen, Charles G., et al. "On Transient Climate Change at the Cretaceous−Paleogene Boundary Due to Atmospheric Soot Injections." *Proceedings of the National Academy of Sciences*, vol. 114, no. 36, 2017, https://doi.org/10.1073/pnas.1708980114.

Biermann, Frank, et al. "Solar Geoengineering: The Case for an International Non-Use Agreement." *WIREs Climate Change*, 17 Jan. 2022, 10.1002/wcc.754. Accessed 21 Jan. 2022.

Black, Benjamin A., et al. "Global Climate Disruption and Regional Climate Shelters after the Toba Supereruption." *Proceedings of the National Academy of Sciences*, vol. 118, no. 29, 2021, https://doi.org/10.1073/pnas.2013046118.

Black, Benjamin A., et al. "Systemic Swings in End-Permian Climate from Siberian Traps Carbon and Sulfur Outgassing." *Nature Geoscience*, vol. 11, no. 12, 2018, pp. 949–954., https://doi.org/10.1038/s41561-018-0261-y.

Brasseur, Orlando, and Tyndall. Atmospheric Chemistry and Global Change, Oxford University Press, 1999.

618 Bostrom, Nick, and Milan M. Cirkovic. *Global Catastrophic Risks*. Oxford University
619 Press, 2008.
620 Cao, Long, et al. "Simultaneous Stabilization of Global Temperature and Precipitation
621 through Cocktail Geoengineering." Geophysical Research Letters, vol. 44, no. 14,
622 2017, pp. 7429–7437., https://doi.org/10.1002/2017gl074281.
623 Cassidy, M., & Mani, L. (2022). Huge volcanic eruptions: time to prepare. In Nature
624 (Vol. 608, Issue 7923, pp. 469–471). Springer Science and Business Media LLC.
625 https://doi.org/10.1038/d41586-022-02177-x
626 Chen J., H. Cui, Y. Xu and Q. Ge (2021) Long-term temperature and sea-level rise
627 stabilization before and beyond 2100: Estimating the additional climate mitigation
628 contribution from China's recent 2060 carbon neutrality pledge. Environ. Res.
629 Lett. 16 074032
630 Chen, J., Cui, H., Xu, Y. & Ge, Q. An Investigation of Parameter Sensitivity of Minimum
631 Complexity Earth Simulator. Atmosphere. 11(1), (2020).
632 Cheng, Andrew F., et al. "AIDA DART Asteroid Deflection Test: Planetary Defense and
633 Science Objectives." *Planetary and Space Science*, vol. 157, 2018, pp. 104–115.,
634 https://doi.org/10.1016/j.pss.2018.02.015.
635 Coupe, Joshua, et al. "Nuclear Winter Responses to Nuclear War Between the United
636 States and Russia in the Whole Atmosphere Community Climate Model Version
637 4 and the Goddard Institute for Space Studies ModelE." *Journal of Geophysical*
638 *Research: Atmospheres*, vol. 124, no. 15, 2019, pp. 8522–8543.,
639 https://doi.org/10.1029/2019jd030509.

Da, Y., Xu, Y. & McCarl, B. Effects of Surface Ozone and Climate on Historical (1980–2015) Crop Yields in the United States: Implication for Mid-21st Century Projection. Environmental and Resource Economics (2021). https://doi.org/10.1007/s10640-021-00629-y.

Denkenberger, David C., and Robert W. Blair. "Interventions That May Prevent or Mollify Supervolcanic Eruptions." *Futures*, vol. 102, 2018, pp. 51–62., https://doi.org/10.1016/j.futures.2018.01.002.

Dreyfus, G. B., Xu, Y., Shindell, D. T., Zaelke, D., & Ramanathan, V. (2022). Mitigating climate disruption in time: A self-consistent approach for avoiding both near-term and long-term global warming. Proceedings of the National Academy of Sciences, 119(22), e2123536119.

Fendley, Isabel M., et al. "Constraints on the Volume and Rate of Deccan Traps Flood Basalt Eruptions Using a Combination of High-Resolution Terrestrial Mercury Records and Geochemical Box Models." *Earth and Planetary Science Letters*, vol. 524, 2019, p. 115721., https://doi.org/10.1016/j.epsl.2019.115721.

Fuglestvedt, J. S., B. H. Samset, and K. P. Shine (2014), Counteracting the climate effects of volcanic eruptions using short-lived greenhouse gases, Geophys. Res. Lett., 41, 8627–8635, doi:10.1002/2014GL061886.

Ganopolski, A., Winkelmann, R. & Schellnhuber, H. Critical insolation–CO2 relation for diagnosing past and future glacial inception. Nature 529, 200–203 (2016). https://doi.org/10.1038/nature16494

661 Hanna, Ryan, et al. “Emergency Deployment of Direct Air Capture as a Response to the
662 Climate Crisis.” *Nature Communications*, vol. 12, no. 1, 2021,
663 https://doi.org/10.1038/s41467-020-20437-0.
664 Hasselmann, K. “Stochastic Climate Models Part I. Theory.” *Tellus*, vol. 28, no. 6, 1976,
665 pp. 473–485., https://doi.org/10.3402/tellusa.v28i6.11316.
666 Hayes, T.S., et al., Critical mineral resources of the United States—Economic and
667 environmental geology and prospects for future supply: U.S. Geological Survey
668 Professional Paper 1802, p. G1–G80, 2017, http://doi.org/10.3133/pp1802G.
669 Hodnebrog, Ø., et al. “Updated Global Warming Potentials and Radiative Efficiencies of
670 Halocarbons and Other Weak Atmospheric Absorbers.” *Reviews of Geophysics*,
671 vol. 58, no. 3, 2020, https://doi.org/10.1029/2019rg000691.
672 IEA (2021), Natural Gas Information: Overview, IEA, Paris
673 https://www.iea.org/reports/natural-gas-information-overview
674 IPCC, 2014: Climate Change 2014: Synthesis Report. Contribution of Working Groups I,
675 II and III to the Fifth Assessment Report of the Intergovernmental Panel on
676 Climate Change [Core Writing Team, R.K. Pachauri and L.A. Meyer (Eds.)].
677 IPCC, Geneva, Switzerland, 151 Pp.
678 Jaccaud, Michel, et al. “Fluorine.” *Ullmanns Encyclopedia of Industrial Chemistry*, 2020,
679 pp. 1–19., https://doi.org/10.1002/14356007.a11_293.pub2.
680 Knott, T.R., et al., 2020, Discovery of two new super-eruptions from the Yellowstone
681 hotspot track (USA): Is the Yellowstone hotspot waning?: *Geology*, v. 48, p. 934–
682 938, https://doi.org/10.1130/G47384.1

683 Li, Mengze, et al. “Tropospheric OH and Stratospheric OH and Cl Concentrations
684 Determined from CH4, CH3Cl, and SF6 Measurements.” *Npj Climate and*
685 *Atmospheric Science*, vol. 1, no. 1, 2018, https://doi.org/10.1038/s41612-018-
686 0041-9.
687 U.S. Geological Survey, 2020, Mineral commodity summaries 2020: U.S. Geological
688 Survey, pp. 60-61., https://doi.org/10.3133/mcs2020.
689 Mills, Michael J., et al. “Multidecadal Global Cooling and Unprecedented Ozone Loss
690 Following a Regional Nuclear Conflict.” *Earth's Future*, vol. 2, no. 4, 2014, pp.
691 161–176., https://doi.org/10.1002/2013ef000205.
692 Mir, Charles El, et al. “A New Hybrid Framework for Simulating Hypervelocity Asteroid
693 Impacts and Gravitational Reaccumulation.” *Icarus*, vol. 321, 2019, pp. 1013–
694 1025., https://doi.org/10.1016/j.icarus.2018.12.032.
695 Morton, Mary Caperton. “Don't Call It a Supervolcano.” *Eos*, 28 Sept. 2021,
696 https://eos.org/features/dont-call-it-a-supervolcano.
697 National Academies of Sciences, Engineering, and Medicine. 2021. *Reflecting Sunlight:*
698 *Recommendations for Solar Geoengineering Research and Research Governance*.
699 Washington, DC: The National Academies Press.https://doi.org/10.17226/25762.
700 Newhall et al., 2018: Anticipating future Volcanic Explosivity Index (VEI) 7 eruptions
701 and their chilling impacts. Geosphere, 14, No. 2, 1-32, doi:10.1130/GES01513.1
702 The Nobel Committee for Physics. “Scientific Background on the Nobel Prize in Physics
703 2021: For Groundbreaking Contributions to Our Understanding of Complex
704 Physical Systems.” The Royal Swedish Academy of Sciences, 2021.

705 Parker, A., et al. “Stopping Solar Geoengineering through Technical Means: A
706 Preliminary Assessment of Counter-Geoengineering.” Earth's Future, vol. 6, no.
707 8, 2018, pp. 1058–1065., https://doi.org/10.1029/2018ef000864.
708 Robock, Alan, et al. “Did the Toba Volcanic Eruption of ∼74 Ka B.P. Produce
709 Widespread Glaciation?” *Journal of Geophysical Research*, vol. 114, no. D10,
710 2009, https://doi.org/10.1029/2008jd011652.
711 Ramachandran, S., et al. “Radiative Impact of the Mount Pinatubo Volcanic Eruption:
712 Lower Stratospheric Response.” *Journal of Geophysical Research: Atmospheres*,
713 vol. 105, no. D19, 2000, pp. 24409–24429.,
714 https://doi.org/10.1029/2000jd900355.
715 Ramanathan, V., Xu, Y. & Versaci, A. Modelling human–natural systems interactions
716 with implications for twenty-first-century warming. Nat Sustain (2021).
717 https://doi.org/10.1038/s41893-021-00826-z
718 Sayyed, M.r.g. “Flood Basalt Hosted Palaeosols: Potential Palaeoclimatic Indicators of
719 Global Climate Change.” *Geoscience Frontiers*, vol. 5, no. 6, 2014, pp. 791–799.,
720 https://doi.org/10.1016/j.gsf.2013.08.005.
721 Scherrer, Kim J. N., et al. “Marine Wild-Capture Fisheries after Nuclear War.”
722 *Proceedings of the National Academy of Sciences*, vol. 117, no. 47, 2020, pp.
723 29748–29758., https://doi.org/10.1073/pnas.2008256117.
724 Self, S., Rampino, M.R., Newton, M.S., Wolff, J.A., 1984. Volcanological study of the
725 great Tambora eruption of 1815. Geology, 12, 659 – 663.

726 Soden, Brian J., et al. “Global Cooling After the Eruption of Mount Pinatubo: A Test of
727 Climate Feedback by Water Vapor.” *Science*, vol. 296, no. 5568, 2002, pp. 727–
728 730., https://doi.org/10.1126/science.296.5568.727.
729 Stenchikov, Georgiy L., et al. “Radiative Forcing from the 1991 Mount Pinatubo
730 Volcanic Eruption.” *Journal of Geophysical Research: Atmospheres*, vol. 103, no.
731 D12, 1998, pp. 13837–13857., https://doi.org/10.1029/98jd00693.
732 Stevenson, D. S., Johnson, C. E., Highwood, E. J., Gauci, V., Collins, W. J., and
733 Derwent, R. G.: “Atmospheric impact of the 1783–1784 Laki eruption: Part I
734 Chemistry modeling”, Atmos. Chem. Phys., 3, 487–507,
735 https://doi.org/10.5194/acp-3-487-2003, 2003.
736 Teller, Edward, Lowell Wood, Hoover Institution, and Roderick Hyde. "Global Warming
737 and Ice Ages:" In The Carbon Dioxide Dilemma, 22. UCRL-JC 135414.
738 Livermore, California: Lawrence Livermore National Laboratory, 1997.
739 Teller, Edward, Roderick Hyde, and Lowell Wood. "Active Climate Stabilization:
740 Practical Physics-Based Approaches to Prevention of Climate Change."
741 Livermore, California: Lawrence Livermore National Laboratory, 2002.
742 Tilmes, Simone, et al. “Sensitivity of Aerosol Distribution and Climate Response to
743 Stratospheric SO2 Injection Locations.” *Journal of Geophysical Research:*
744 *Atmospheres*, vol. 122, no. 23, 2017, https://doi.org/10.1002/2017jd026888.
745 Tilmes, Simone, et al. “CESM1(WACCM) Stratospheric Aerosol Geoengineering Large
746 Ensemble Project.” *Bulletin of the American Meteorological Society*, vol. 99, no.
747 11, 2018, pp. 2361–2371., https://doi.org/10.1175/bams-d-17-0267.1.

748 Timmreck, Claudia, et al. “Aerosol Size Confines Climate Response to Volcanic Super-
749 Eruptions.” *Geophysical Research Letters*, vol. 37, no. 24, 2010,
750 https://doi.org/10.1029/2010gl045464.
751 Timmreck, Claudia, et al. “Climate Response to the Toba Super-Eruption: Regional
752 Changes.” *Quaternary International*, vol. 258, 2012, pp. 30–44.,
753 https://doi.org/10.1016/j.quaint.2011.10.008.
754 Timmreck, C. and Graf, H.-F.: The initial dispersal and radiative forcing of a Northern
755 Hemisphere mid-latitude super volcano: a model study, Atmos. Chem. Phys., 6,
756 35–49, https://doi.org/10.5194/acp-6-35-2006, 2006
757 Toon, Owen B., et al. “Environmental Perturbations Caused by the Impacts of Asteroids
758 and Comets.” *Reviews of Geophysics*, vol. 35, no. 1, 1997, pp. 41–78.,
759 https://doi.org/10.1029/96rg03038.
760 Toon, Owen B., et al. “Environmental Consequences of Nuclear War.” *AIP Conference*
761 *Proceedings,* 2014, https://doi.org/10.1063/1.4876320.
762 Toon, Owen B., et al. “Rapidly Expanding Nuclear Arsenals in Pakistan and India
763 Portend Regional and Global Catastrophe.” *Science Advances*, vol. 5, no. 10,
764 2019, https://doi.org/10.1126/sciadv.aay5478.
765 United Nations Environment Programme and International Energy Agency (2020).
766 Cooling Emissions and Policy Synthesis Report: Benefits of cooling efficiency
767 and the Kigali Amendment. UNEP, Nairobi and IEA, Paris. (pdf, UNEP press
768 release)

769 Velders, G. J. M., et al. “The Large Contribution of Projected HFC Emissions to Future
770 Climate Forcing.” Proceedings of the National Academy of Sciences, vol. 106,
771 no. 27, 2009, pp. 10949–10954., https://doi.org/10.1073/pnas.0902817106.
772 Velders, Guus J.m., et al. “Future Atmospheric Abundances and Climate Forcings from
773 Scenarios of Global and Regional Hydrofluorocarbon (HFC) Emissions.”
774 Atmospheric Environment, vol. 123, 2015, pp. 200–209.,
775 https://doi.org/10.1016/j.atmosenv.2015.10.071.
776 Vellekoop, J., et al. “Rapid Short-Term Cooling Following the Chicxulub Impact at the
777 Cretaceous-Paleogene Boundary.” *Proceedings of the National Academy of*
778 *Sciences*, vol. 111, no. 21, 2014, pp. 7537–7541.,
779 https://doi.org/10.1073/pnas.1319253111.
780 Visioni, D., MacMartin, D. G., Kravitz, B., Tilmes, S., Mills, M. J., Richter, J. H., and
781 Boudreau, M. P. (2019). "Seasonal Injection Strategies for Stratospheric Aerosol
782 Geoengineering". *Geophysical Research Letters*, 1-10.
783 https://doi.org/10.1029/2019GL083680
784 Wilcox, Brian. “Defending Human Civilization from Supervolcanic Eruptions.” 2015,
785 https://scienceandtechnology.jpl.nasa.gov/sites/default/files/documents/Defending
786 CivilizationFromSupervolcanos20151015.pdf.
787 Wilson, Colin J. N., et al. “No Single Model for Supersized Eruptions and Their Magma
788 Bodies.” *Nature Reviews Earth & Environment*, vol. 2, no. 9, 2021, pp. 610–627.,
789 https://doi.org/10.1038/s43017-021-00191-7.

Xu, Y., et al. “The Role of HFCs in Mitigating 21st Century Climate Change.” *Atmospheric Chemistry and Physics*, vol. 13, no. 12, 2013, pp. 6083–6089., https://doi.org/10.5194/acp-13-6083-2013.

Xu, Y., et al. “Climate Engineering to Mitigate the Projected 21st-Century Terrestrial Drying of the Americas: a Direct Comparison of Carbon Capture and Sulfur Injection.” *Earth System Dynamics*, vol. 11, no. 3, 2020, pp. 673–695., https://doi.org/10.5194/esd-11-673-2020.

Xu, Y., and V. Ramanathan (2017), Well below 2 °C: Mitigation strategies for avoiding dangerous to catastrophic climate changes. Proc. Natl. Acad. Sci. , doi:10.1073/pnas.1618481114 .

800

801 **Table 1. A list of F-gas candidates ranked by lifetimes (0.5 to 3.2 years). The five rows in**
802 **boldface are compounds selected for further modeling analysis due to their higher**
803 **GWP/lifetime ratio (A-E, ranked by this ratio [large to small]).**

804

Chemical identifier	Formula (+ Molar weight)	Lifetime (yr)	Radiative Efficiency ($Wm^{-2}ppb^{-1}$)	GWP100	ratio = GWP100 /lifetime
HFC-152	CH_2FCH_2F	0.5	0.05	23	46
1,3,3,4,4,5,5-heptafluoro cyclopentane	cyc (-$CF_2CF_2CF_2CF$=CH-)	*0.6*	*0.21*	47	78
1,3,3,4,4-pentafluorocyclobutene (A)	**cyc (-CH=CFCF$_2$CF$_2$-), (**144 g/mol)	**0.7**	***0.27***	**97**	**139**
Hexafluorocyclobutene (B)	**cyc (-CF=CFCF$_2$CF$_2$-), (**162 g/mol)	***1***	***0.3***	**132**	**132**
HFC-263fb	$CH_3CH_2CF_3$	1.1	*0.1*	78	71
Octafluorocyclopentene	cyc (-$CF_2CF_2CFCF_2CF_2$-)	1.1	*0.25*	82	75
1,1,2,2,3,3-hexafluorocyclopen	cyc (-$CF_2CF_2CF_2CH_2CH_2$-)	*1.6*	*0.2*	126	79

tane					
HFC-152a (C)	**CH_3CHF_2 (**66 g/mol)	**1.6**	**0.1**	**172**	**108**
HFC-41 (E)	**CH_3F (**34 g/mol)	**2.8**	**0.02**	**142**	**50.7**
1,1,2,2,3,3,4-heptafluorocyclopentane	cyc (-$CF_2CF_2CF_2CHFCH_2$-)	2.8	0.24	243	86.8
HFC-245ea	$CHF_2CHFCHF_2$	3.2	0.16	267	83.4
HFC-245eb (D)	**$CH_2FCHFCF_3$ (**134 g/mol)	**3.2**	**0.2**	**341**	**106.6**
(4R,5R)-1,1,2,2,3,3,4,5-octafluorocyclopentane	trans-cyc (-$CF_2CF_2CF_2CHFCHF$-)	3.2	0.26	271	84.7

805

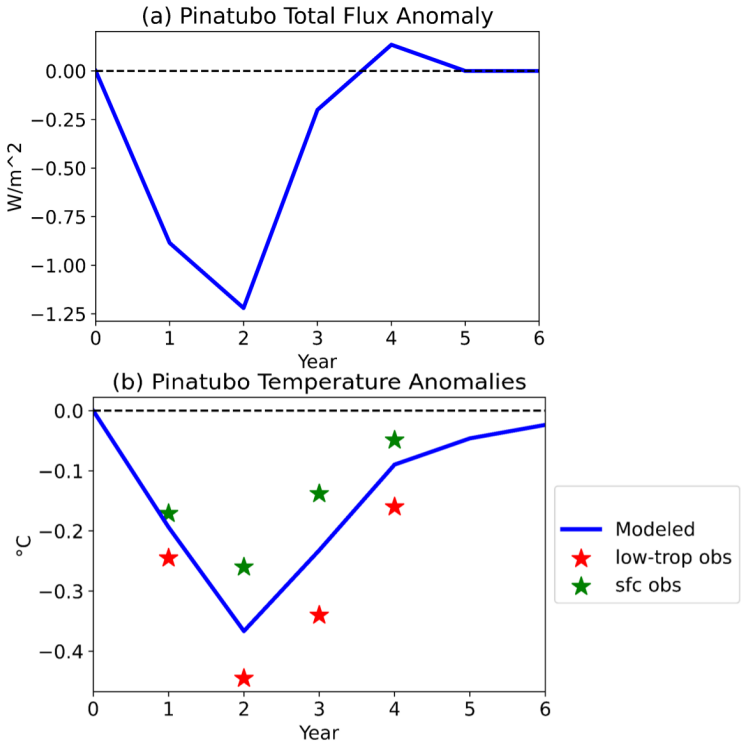

Figure 1. (a) TOA radiative flux anomaly following the Pinatubo eruption, calculated from shortwave and longwave monthly observations (Figure 1 in Soden et al., 2002). (b) Surface temperature response in our model, compared to the lower troposphere and surface observations (Soden et al., 2002; Bender et al., 2010). Year Zero on the x-axis represents June 1990 to May 1991, the year preceding the eruption in June 1991.

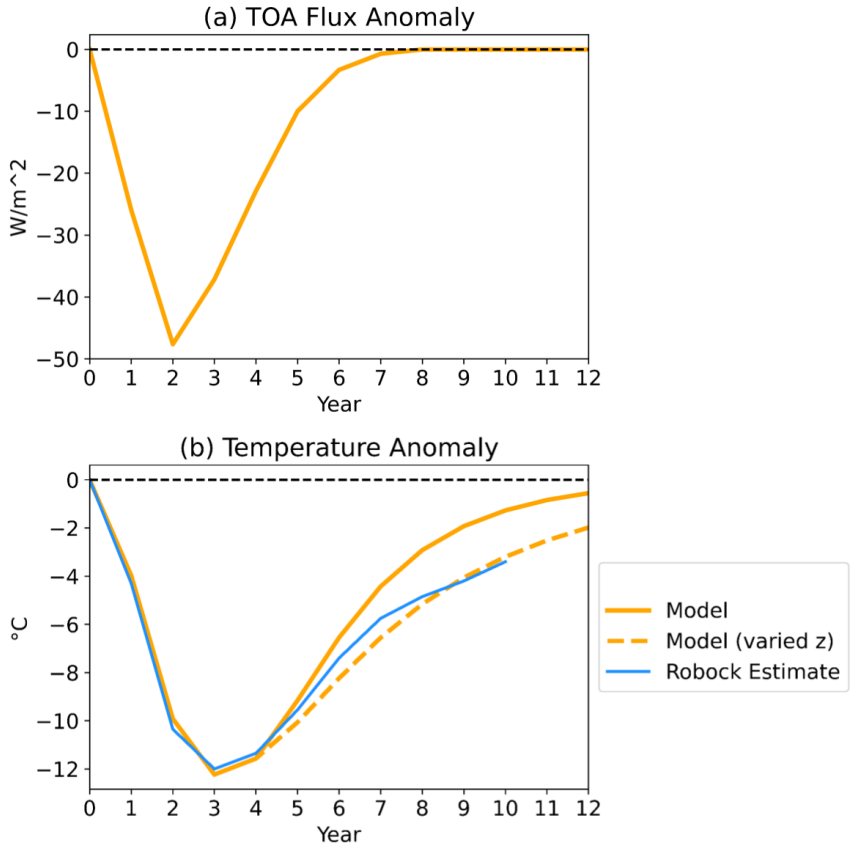

Figure 2. (a) TOA radiative forcing following a 2-Gt SO_2 injection (converted from the shortwave surface forcing estimates in Figure 4 of Robock et al., 2009). (b) Simulated global surface cooling (orange solid line) using the forcing estimates in (a), which is compared with Robock et al. (2009) (blue solid line). The orange dash line is also simulated by our model, but assuming the effective ocean depth (z) increases from 50 to 80 meters in Year 5.

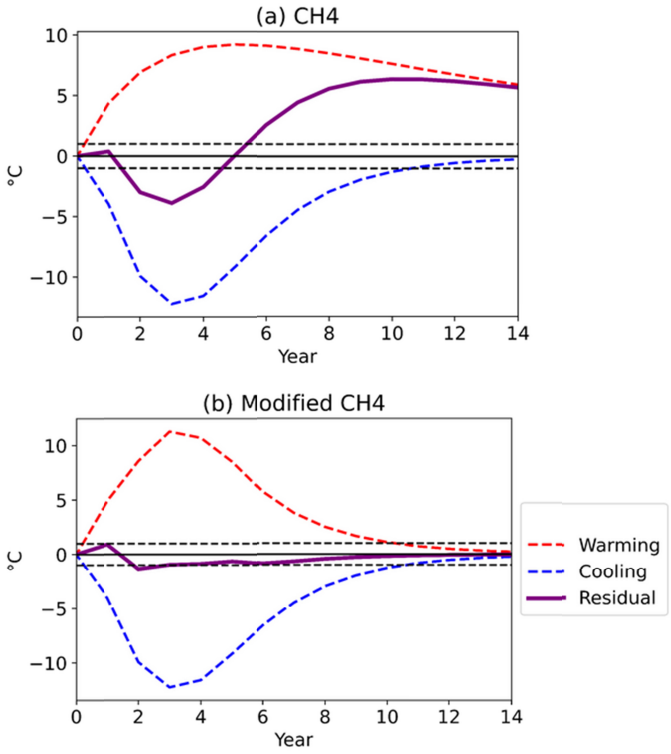

Figure 3. (a) Supervolcanic cooling mitigation via a hypothetical 200 Gt CH_4 emission in Year 1, which is clearly infeasible. The blue dashed line is cooling due to the volcanic eruption. The red dashed line is heating due to GHG release. The solid purple line represents the residual (i.e., summation of cooling and heating). Targeted [-1°C, 1°C] limits are shown as horizontal dashed lines. (b) Similar mitigation via a 6 Gt "CH_4"-like emission (with stronger radiative efficiency and shorter lifetime) in Year 1, followed by 3.5 Gt releases in Years 2 and 3.

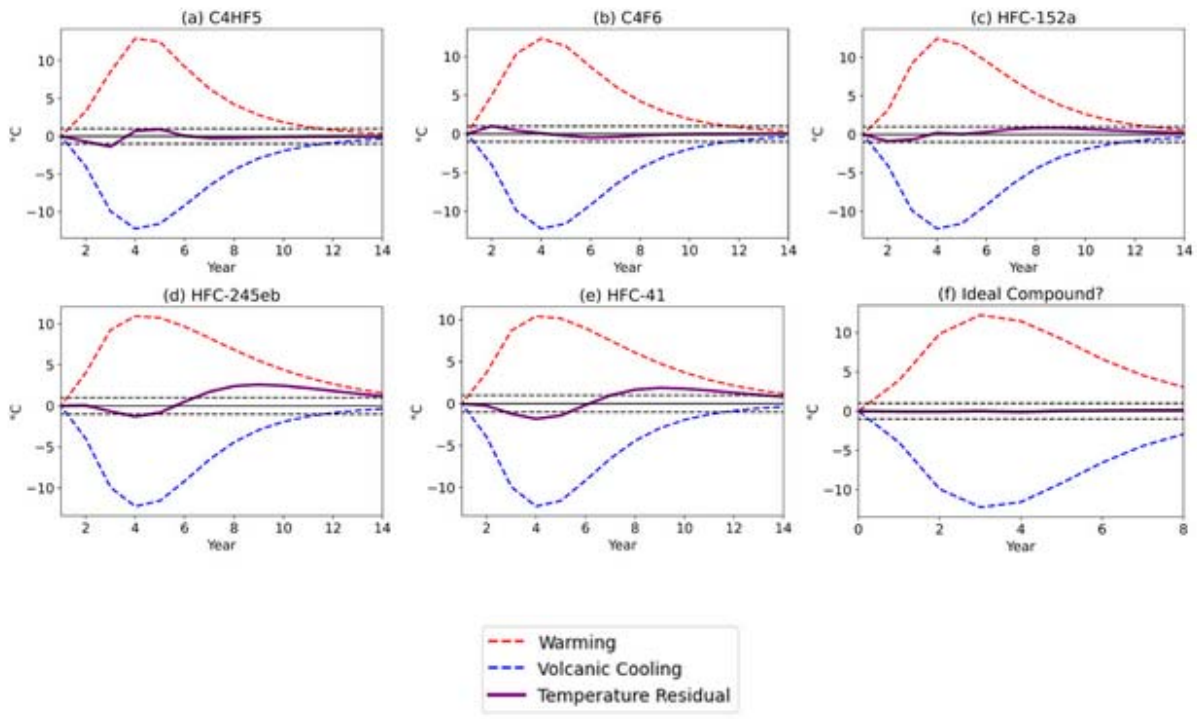

827

828 **Figure 4. Simulated volcanic cooling and warming offset by F-gas emission. (a) C_4HF_5; (b)**
829 **C_4F_6; (c) HFC-152a; (d) HFC-245eb; (e) HFC-41 (CH_3F); and (f) a possible compound with**
830 **ideal characteristics. The blue dashed line is cooling due to volcanic eruption. The red**
831 **dashed line is heating due to F-gases. Each purple solid line represents the residual (net**
832 **temperature effect), which aims to fall mostly into the 1ºC range indicated by the**
833 **horizontal dashed lines. Note that in (f) the timeline is shortened to Year 0 to 8 to**
834 **demonstrate a clear optimal counterbalancing by the 'ideal' compound.**

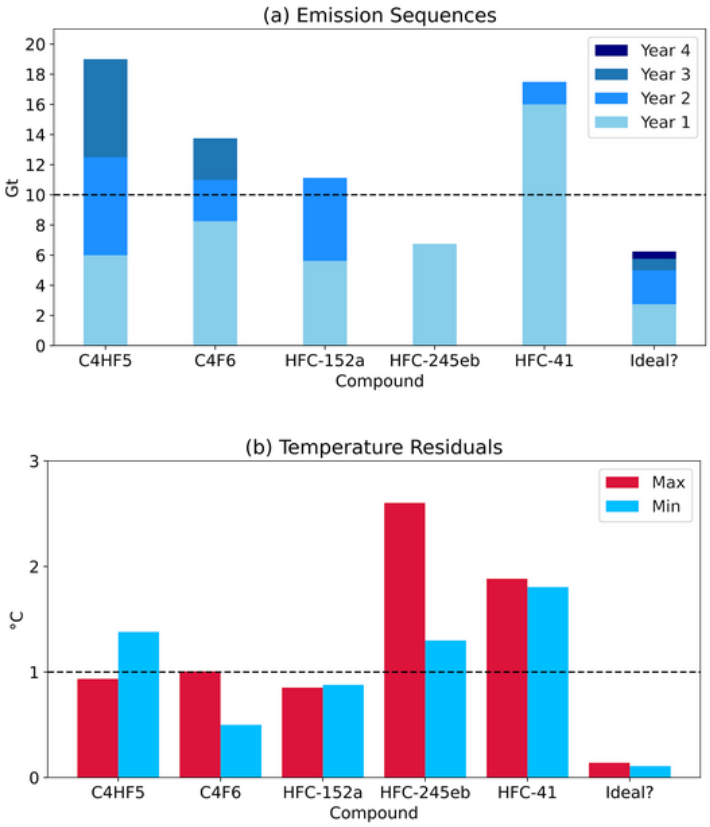

Figure 5. (a) The sequencing of annual emission of the five identified compounds, as well as the "ideal" compound. The sequence of emission is constructed via simple model runs with optimized results shown in Figure 4. (b) The range of temperature residuals as seen in Figure 4, which is targeted to be kept below 1ºC.

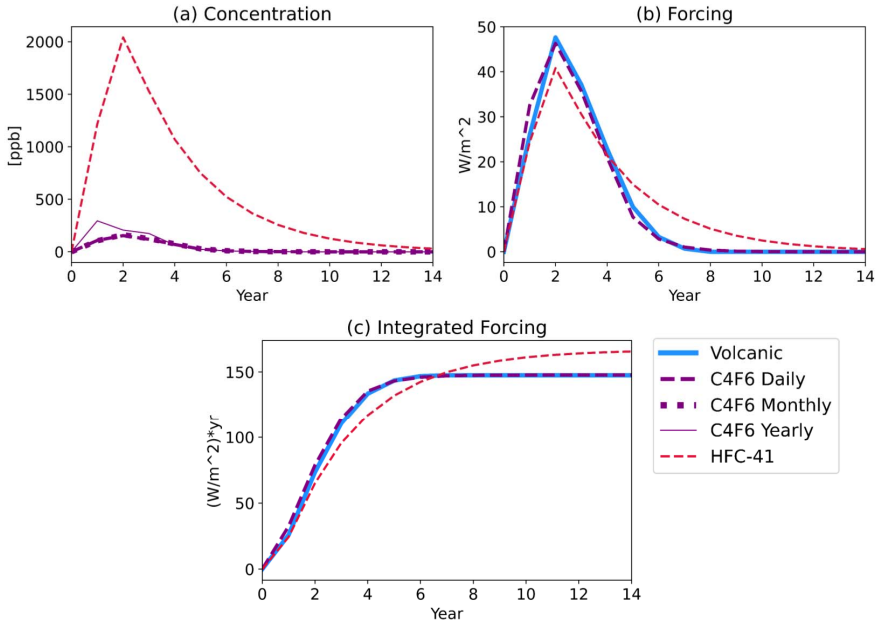

Figure 6.

(a) Simulated average atmospheric concentrations of C_4F_6 (Compound B, purple dashed line C_4F_6 daily) and HFC-41 (Compound E, red dashed line). Results using monthly (purple dot-dash line) and yearly (purple solid thin line) time steps, respectively, are also included as a robustness check for the shorter-lived C_4F_6. The monthly time steps show very good agreement with the default results using daily steps, while the yearly time steps produce a concentration biased high.

(b) and (c): simulated radiative forcing and integrated radiative forcing, respectively, of C_4F_6 (Compound B, purple dashed line C_4F_6 daily) and HFC-41 (Compound E, red dashed line). Volcanic forcing (blue solid line) as in Figure 2 is shown again for reference.